ELSEVIER

www.elsevier.nl/locate/jorganchem

Journal of Organometallic Chemistry 589 (1999) 38–49

Journal of Organometallic Chemistry

The ferrocene moiety as a structural probe: redox and structural properties of ferrocenoyl-oligoprolines Fc–Pro_n–OBzl ($n = 1–4$) and Fc–Pro_2–Phe–OBzl

Heinz-Bernhard Kraatz [a,b,*], Donald M. Leek [a], Abdelaziz Houmam [a], Gary D. Enright [a], Janusz Lusztyk [a], Danial D.M. Wayner [a]

[a] *Steacie Institute of Molecular Sciences, National Research Council of Canada, 100 Sussex Drive, Ottawa, Ont. K1A 0R6, Canada*
[b] *Department of Chemistry, 110 Science Place, University of Saskatchewan, Saskatoon, Sask. S7N 5C9, Canada*

Received 12 February 1999; received in revised form 20 April 1999

Abstract

The preparations of the five ferrocenoyl-oligopeptides, Fc–Pro–OBzl (**1**), Fc–Pro_2–OBzl (**2**), Fc–Pro_3–OBzl (**3**), Fc–Pro_4–OBzl (**4**) and Fc–Pro_2–Phe–OBzl (**5**) are described. Crystallographic studies show that the Fc-oligoprolines **1**–**4** adopt a helical polyproline II structure having all prolines in a mutually *trans*-conformation. This structure is maintained in MeCN and $CHCl_3$ solutions, as was shown by NMR methods. Chemical and magnetic similarities among the proline residues render spectral assignment by conventional 1D ^{1}H-NMR spectroscopy impossible. However, a combination of 2D NMR techniques allowed us to unequivocally assign all signals. The redox potential of the Fc-group attached to the oligoproline chain is sensitive to the sequence and length of the oligopeptide. With growing peptide length, the molecule becomes easier to oxidize.

Keywords: Ferrocene; Proline; Oligopeptide; NMR; Redox behavior; Crystal structure; Bioorganometallic

1. Introduction

Electron transfer (ET) processes are key steps in many enzymatic reactions involving the reduction or oxidation of bound substrates. In the utilization of light in green plants, redox charge separation is of fundamental importance [1]. ET and/or energy transfer that follows the initial light absorption are influenced by the nature of the chromophores, the redox active quenchers, and the intervening medium (solvent and/or spacers). Progress has been made in understanding ET processes by making use of modified metalloproteins [2]. However, in these experimental studies distances and relative orientations between an electron donor D and an acceptor A have not been rigorously established. Since the matrix separating redox sites in proteins is a complex system containing various structural elements, no information about specific structural effects can be obtained from these investigations. Theoretical studies by Beratan and coworkers [3] clearly show that peptides having a β-sheet structure are more effective in ET than α-helical peptides. Experimental results by Gray and coworkers suggest that primary, secondary and tertiary structures of a protein are all important for modifying ET rates. Furthermore, H-bonding in proteins influences ET rates [4]. Studies of ET in peptides have concentrated on understanding how ET properties are modified by D–A separations [5]. It was noted that high flexibility of the oligopeptide linker results in a lower observed ET rate [5a]. Recently, Fox and Galoppini [5l,m] have observed a directional anisotropy of ET rates and have attributed this to field effects generated by the alignment of the amide C=O dipoles in the peptide.

In our studies, we are interested in the ET properties of rigid and flexible peptide assemblies, addressing the role of the peptidic backbone in ET processes and assessing the influence of amino acid side chains in

* Corresponding author.
E-mail address: kraatz@skyway.usask.ca (H.-B. Kraatz)

0022-328X/99/$ - see front matter
PII: S0022-328X(99)00300-9

modifying the ET characteristics of a peptide chain. We make use of the ferrocenoyl (Fc) moiety as an electrochemical probe, which is sensitive to small structural changes [6]. We have been making use of the carbodiimide method allowing us to introduce the ferrocene moiety into a peptidic environment under very mild conditions [7]. In the past year, various groups have reported similar amide couplings of ferrocene derivatives to amino acids and other substrates [8]. Since oligoprolines have been studied in great detail, we have chosen to begin our investigation with Fc-oligoprolines to establish a 'baseline' for the redox behavior of our Fc-oligopeptides from which we can proceed to study other structurally diverse peptides. Here we present our results showing for the first time that the oxidation of a Fc moiety attached to an oligoproline chain is sensitive to the chain length, its secondary structure and to the amino acid sequence.

2. Experimental

2.1. General

Ferrocene carboxylic acid, dicyclohexyl carbodiimide (DCC), trifluoroacetic acid (TFA) and hydroxybenzotriazole (HOBt) (Aldrich), and Boc–Pro–OH, H–Pro-OBz·HCl (Nova-Biochem) were used as received. The peptides Boc–Pro_n–OBzl ($n = 2$–4) were prepared according to published procedures [16]. All solvents were used as received without further treatment. Routine ^{1}H- and ^{13}C-NMR spectra were recorded at 200.132 and 50.323 MHz, respectively on a Bruker AC 200 NMR spectrometer. All chemical shifts (δ) are reported in ppm and coupling constants (J) in Hz. The ^{1}H- and ^{13}C-NMR chemical shifts are relative to tetramethylsilane ($\delta = 0$ ppm), which was added as an internal standard. All measurements were carried out at 293 K unless otherwise specified. Elemental analyses were carried out at the NRCs Institute for Biology, Ottawa, Canada.

2.2. General procedure for the synthesis of ferrocenoyl-oligoprolines

2.2.1. Example: preparation of Fc–Pro_2–OBzl (**2**)

2.2.1.1. Method A. Fc–Pro–OBzl was prepared as described earlier [7]. A slow stream of hydrogen gas was bubbled through a vigorously stirring reaction mixture of Fc–Pro–OBzl (0.2 g) and 5% Pd/C (0.2 g) in MeOH (40 ml). The progress of the reaction was followed by TLC (silica, CH_2Cl_2) and was complete after 20 min. Pd/C was removed by filtration. Water (10 ml) was added and the pH of the solution was adjusted to pH 2. The product was extracted with CH_2Cl_2 (3×50 ml) and then recrystallized from CH_2Cl_2–Et_2O (1:1) to give thin orange plates of X-ray quality. Fc–Pro–OH (**1**-OH) $C_{16}H_{17}O_3NFe$: MW = 327. Found by ESMS 328.1. **1**-OH (35 mg) was then treated with DCC (22 mg), HOBt (16 mg) and H–Pro–OBzl·HCl (27 mg) in CH_2Cl_2 at room temperature (r.t). Orange–red Fc–Pro_2–OBzl was isolated by standard work-up described earlier. Yield, 65%. Thin orange needles were obtained by slow evaporation of CH_2Cl_2 from a saturated solution at r.t.

2.2.1.2. Method B. Boc–Pro_2–OBzl (0.4 g, 0.99 mmol) was treated with TFA (5 ml) for 1 h to the free base H–Pro_2–OBzl. Excess TFA was removed in vacuo. FcCOOH (0.23 g, 0.99 mmol) was dissolved in CH_2Cl_2 (10 ml). The solution was cooled with an ice bath and DCC (0.22 g, 1.1. mmol) and HOBt (0.13 g, 1.1 mmol) were added. H–Pro_2–OBzl was added after 30 min to the stirring reaction mixture of FcCOOH, DCC and HOBt. The product was isolated by standard work-up, described earlier [7]. Yield, 75%. Spectroscopic properties were identical to those of Fc–Pro_2–OBzl obtained by method A (see below).

2.3. Spectroscopic data for **2**

MW for $C_{28}H_{30}N_2O_4Fe$. Calc: 514.4. Found: 515.2 $[M+1]^+$. ^{1}H-NMR (δ ppm, $CDCl_3$): 7.34 (5H, br m, aromatic H of Ph), 5.15 (2H, second-order m, OCH_2Ph), 4.82 (2H, m, H *ortho* to carboxy group on Cp ring overlapping with signal due to NC*H*(R)C(O)), 4.71 (2H, m, overlapping signals due to NC*H*(R)C(O) and H *ortho* to carboxy group on Cp ring), 4.31 (2H, s, H *meta* to carboxy group on Cp ring), 4.28 (5H, s, Hs of unsubstituted Cp ring), 3.9–3.6 (4H, m, signals due to the two diastereotopic Hs of –NC*H*$_2$–), 2.2–1.8 (ca. 8H, m, two signals due to the two diastereotopic Hs adjacent to stereocenter –C(H)C*H*$_2$C*H*$_2$C*H*$_2$N, overlapping with signal due to one of the H of the –NCH$_2$C*H*$_2$CH$_2$– group). ^{13}C{^{1}H}-NMR (δ ppm, $CDCl_3$): 172.3 (C=O), 170.9 (C=O), 169.4 (C=O), 135.8 (s, quartenary C of Ph), 128.5 (br s, Ph), 128.2 (br s, Ph), 127.5 (br s, Ph), 71.3 (s, C on substituted Cp), 70.4 (s, C on substituted Cp), 70.2 (s, C on substituted Cp), 69.7 (s, unsubstituted Cp ring of Fc), 69.5 (s, C on substituted Cp), 66.8 (s, − ve DEPT, O*C*H$_2$Ph), 59.1 (s, + ve DEPT, N(H)–*C*H–C(O) of proline ring next to Fc), 58.8 (s, + ve DEPT, N(H)–*C*H–C(O) of Pro next to OBzl group), 49.1 (s, − ve DEPT, N(H)–*C*H$_2$–CH$_2$ of Pro next to Fc), 46.6 (s, − ve DEPT, N(H)–*C*H$_2$–CH$_2$ of Pro next to OBzl), 28.8 (s, − ve DEPT, –*C*H$_2$– Pro next to Fc), 27.8 (s, − ve DEPT, –*C*H$_2$– Pro next to OBzl), 25.5 (s, − ve DEPT, –*C*H$_2$– Pro next to Fc), 24.9 (s, − ve DEPT, –*C*H$_2$– Pro next to Fc).

2.4. Spectroscopic data for Fc–Pro_3–OBzl (3)

Complex **3** was synthesized from ferrocene carboxylic acid and Boc–Pro_3–OBzl according to method B. Yield, 70%. MW for $C_{33}H_{37}N_3O_5Fe$: Calc: 611.5. Found: 612.3 $[M+1]^+$. ^{1}H-NMR (δ ppm, $CDCl_3$): 7.38 (5H, br m, aromatic H of Ph), 5.13 (2H, second-order m, OCH_2Ph), 4.84–4.61 (5H, m, H *ortho* to carboxy group on Cp ring overlapping with signal due to NC*H*(R)C(O)), 4.33 (2H, s, H *meta* to carboxy group on Cp ring), 4.26 (5H, s, Hs of unsubstituted Cp ring), 3.93–3.61 (6H, m, signals due to the two diastereotopic Hs of –NCH_2), 2.30–1.80 (12H, m, two signals due to the two diastereotopic Hs adjacent to stereocenter –C(H)CH_2CH_2CH_2N–, overlapping with signal due to one of the H of the –NCH_2CH_2 CH_2– group). ^{13}C{^{1}H}-NMR (δ ppm, $CDCl_3$): 172.0 (C=O), 170.7 (C=O), 170.5 (C=O), 169.2 (C=O), 135.6 (s, quartenary C of Ph), 128.4 (br s, Ph), 128.2 (br s, Ph), 71.2 (s, C on substituted Cp), 70.2 (s, C on substituted Cp), 70.1 (s, C on substituted Cp), 69.6 (s, unsubstituted Cp ring of Fc), 66.7 (s, − ve DEPT, O*C*H_2Ph), 59.2 (s, + ve DEPT, N(H)–*C*H–C(O) of proline ring next to Fc), 58.6 (s, + ve DEPT, N(H)–*C*H–C(O) of 2nd Pro from Fc), 57.7 (s, + ve DEPT, N(H)–*C*H–C(O) of Pro next to OBzl group), 48.6 (s, − ve DEPT, N(H)–*C*H_2–CH_2 of Pro next to Fc), 46.8 (s, − ve DEPT, N(H)–*C*H_2–CH_2 of 2nd Pro from Fc), 46.5 (s, − ve DEPT, N(H)–*C*H_2–CH_2 of Pro next to OBzl), 28.7 (s, − ve DEPT, –*C*H_2– Pro next to Fc), 27.9 (s, − ve DEPT, –*C*H_2– 2nd Pro from Fc), 27.7 (s, − ve DEPT, –*C*H_2– Pro next to OBzl), 25.5 (s, − ve DEPT, –*C*H_2– Pro next to Fc), 24.7 (br s, –ve DEPT, –*C*H_2– of other two Pro).

2.5. Spectroscopic data for Fc–Pro_4–OBzl (4)

Complex **4** was synthesized from ferrocene carboxylic acid and Boc–Pro_4–OBzl according to method B. Yield, 65%. MW for $C_{38}H_{44}N_4O_6Fe$: Calc: 708.6. Found: 709.3 $[M+1]^+$. ^{1}H-NMR (δ ppm, $CDCl_3$): 7.33 (5H, br m, aromatic H of Ph), 5.12 (2H, second-order m, OCH_2Ph), 4.83–4.70 (6H, m, H *ortho* to carboxy group on Cp ring overlapping with signal due to NC*H*(R)C(O)), 4.33 (2H, s, H *meta* to carboxy group on Cp ring), 4.27 (5H, s, Hs of unsubstituted Cp ring), 3.91–3.54 (8H, m, signals due to the two diastereotopic Hs of –NCH_2), 2.21–1.89 (16H, m, two signals due to the two diastereotopic Hs adjacent to stereocenter C(H)CH_2CH_2CH_2N–, overlapping with signal due to one of the H of the –NCH_2CH_2CH_2– group). ^{13}C{^{1}H}-NMR (δ ppm, $CDCl_3$): 172.0 (C=O), 170.5 (C=O), 170.4 (C=O), 169.4 (C=O), 128.5 (br s, Ph), 128.2 (br s, Ph), 71.3 (s, C on substituted Cp), 70.2 (s, C on substituted Cp), 69.7 (s, unsubstituted Cp ring of Fc), 66.8 (s, − ve DEPT, O*C*H_2Ph), 59.2 (s, + ve DEPT, N(H)–*C*H–C(O) of proline ring next to Fc), 58.7 (s, + ve DEPT, N(H)–*C*H–C(O) of 2nd Pro from Fc), 57.9 (s, + ve DEPT, N(H)–*C*H–C(O) of 3rd Pro from Fc), 57.7 (s, + ve DEPT, N(H)–*C*H–C(O) of Pro next to OBzl group), 48.6 (s, − ve DEPT, N(H)–*C*H_2–CH_2 of Pro next to Fc), 47.1 (s, − ve DEPT, N(H)–*C*H_2–CH_2 of 2nd Pro from Fc), 46.8 (s, − ve DEPT, N(H)–*C*H_2–CH_2 of 3rd Pro from Fc), 46.4 (s, − ve DEPT, N(H)–*C*H_2–CH_2 of Pro next to OBzl), 29.7 (s, − ve DEPT, –*C*H_2– Pro next to Fc), 28.7 (s, − ve DEPT, –*C*H_2– 2nd Pro from Fc), 28.0 (s, − ve DEPT, –*C*H_2– 3rd Pro from Fc), 27.8 (s, − ve DEPT, –*C*H_2– Pro next to OBzl), 25.7 (s, − ve DEPT, –*C*H_2– Pro next to Fc), 24.8 (br s, − ve DEPT, –*C*H_2– of other two Pro), 24.6 (s, − ve DEPT, –*C*H_2– Pro next to OBzl).

2.6. Spectroscopic data for Fc–Pro_2Phe–OBzl (5)

Complex **5** was synthesized from Boc–Pro_2Phe–OBzl and ferrocene carboxylic acid according to method B. Yield, 73%. MW for $C_{37}H_{39}N_3O_5Fe$: Calc: 661.6. Found: 662.3 $[M+1]^+$. ^{1}H-NMR (δ ppm, $CDCl_3$): 8.34 (1H, d, $J=7.4$ Hz), 7.33 (5H, br s, aromatic H of Ph), 7.28 (5H, br s, aromatic H of Ph), 5.15 (2H, second-order m, OCH_2Ph), 4.87 (1H, m, H *ortho* to carboxy group on Cp), 4.78 (1H, m, H *ortho* to carboxy group on Cp), 4,71 (1H, m, C*H* of Phe), 4.44 (2H, br s, H *meta* to carboxy group on Cp ring, ring overlapping with signal due to NC*H*(R)C(O) of proline ring next to Fc), 4.33 (5H, s, Hs of unsubstituted Cp ring, signal is overlapping with signal due to NC*H*(R)C(O) of proline ring next to Phe), 3.96–3.89 (2H, m, signals due to the two diastereotopic Hs of –NCH_2 of proline ring next to Fc), 3.43–3.25 (4H, m, signals due to the two diastereotopic Hs of –NCH_2 of proline ring next to Phe, overlapping with signals of CH_2Ph of Phe), 2.31–0.90 (8H, m, CH_2 protons). ^{13}C{^{1}H}-NMR (δ ppm, $CDCl_3$): 176.3 (C=O), 171.2 (C=O), 170.1 (C=O), 169.7 (C=O), 135.6 (s, quartenary C of Ph), 129.2 (s, quartenary C of Ph), 129.8, 129.2, 128.9 (br), 128.6, 127.9, 72.0 (s, C on substituted Cp), 71.5 (s, 2C on substituted Cp), 70.3 (s, unsubstituted Cp ring of Fc overlapping with C on substituted Cp), 61.0 (s, + ve DEPT, N(H)–*C*H–C(O) of proline ring next to Fc), 61.4 (s, + ve DEPT, N(H)–*C*H–C(O) of proline ring next to Phe), 56.4 (s, + ve DEPT, N(H)–*C*H–C(O) of Phe), 49.3 (s, − ve DEPT, N(H)–*C*H_2– of Pro next to Fc), 47.2 (s, − ve DEPT, N(H)–*C*H_2– of Pro next to Phe), 39.9 (s, − ve DEPT, *C*H_2Ph of Phe), 32.0 (s, − ve DEPT, CH–*C*H_2– Pro next to Phe), 28.5 (s, − ve DEPT, CH–*C*H_2– Pro next to Fc), 26.2 (s, − ve DEPT, NCH_2–*C*H_2– Pro next to Fc), 21.9 (s, − ve DEPT, NCH_2–*C*H_2– Pro next to Phe).

2.7. Electrochemistry

Cyclic voltammetry experiments were carried out using an EG&G model 173 potentiostat with model 179 coulometer and a model 175 universal programmer. All measurements were made at r.t. (20 ± 1°C) in a standard three-electrode cell with a 3 mm diameter glassy carbon working electrode with Pt wire counter electrode and repeated at least three times. The reference electrode consisted of a silver wire in a 0.1 M solution of $^{n}Bu_4N^+ClO_4^-$ in MeCN separated from the solution by a cracked glass seal. Samples were purged with argon prior to each measurement. Ferrocene was added to the solution as an internal reference. A scan rate of 100 mV s^{-1} was employed for all measurements. All potentials are reported with respect to the ferrocene/ferrocenium redox couple ($E° = 0.44$ V vs. SCE, in MeCN; $\Delta E_p = 80$ mV at a scan rate of 100 mV s^{-1}). All electrochemical potentials are fully reversible. The ratio of the forward to reverse scan peak currents are close to 1 (± 0.05).

2.8. X-ray crystallography

Suitable crystals of **1**-OH, **2**, **3**, **4** and **5**-OH were obtained from CH_2Cl_2 by slow evaporation at -20°C and mounted on glass fibres using epoxy resin. Data for **1**-OH, **3**, **4** and **5**-OH were measured using a Siemens Smart CCD diffractometer Mo–K_α radiation (graphite monochromated) using ω-scans. For complex **2**, data were measured on an Enraf–Nonius CAD4 diffractometer with Cu–K_α radiation (graphite monochromated) using ω-scans. All structures were solved by direct methods using the SHELXTL [9] (**1**-OH, **2**, **3**, **4**) or NRCVAX [10] (**5**-OH) program packages. For **2**, only the Fe and O atoms were refined anisotropically, while all other atoms were refined isotropically using full-matrix least-squares to give $R = 0.1008$, $R_w = 0.2325$ for 553 observed reflections [$I > 2\sigma(I)$]. The phenyl groups for **2** and **3** were constrained to a regular hexagon. For **1**, **3**, and **4**, all non-hydrogen atoms were refined anisotropically using full-matrix least-squares to give the final R values (see Table 1). The thermal motions in the benzyl group for **3** are extremely large and are chiefly responsible for the high residual. For **5**-OH, all non-hydrogen atoms were refined anisotropically using full-matrix least-squares to give final R values of $R = 0.075$, $R_w = 0.071$ for 6248 observed reflections [$I > 2.5\sigma(I)$]. All crystallographic details have been summarized in Table 1.

2.9. NMR studies of Fc–Pro_3–OBzl (3)

NMR spectra were recorded on a Bruker DRX-400 spectrometer using a 5 mm Z-gradient inverse probe and a 5 mm broadband observe probe. The ^1H spectrum was recorded with a 30° pulse, a spectral width of 8220 Hz and 64 scans. The ^{13}C spectrum was recorded with a 30° pulse, a spectral width of 31 800 Hz and 48 000 scans. Standard Bruker pulse sequences were

Table 1
Crystal data for Fc–Pro–OH (**1**-OH), Fc–Pro_2–OBzl (**2**), Fc–Pro_3–OBzl (**3**), Fc–Pro_4–OBzl (**4**) and Fc–Pro_2Phe–OH (**5**-OH)

Compound	**1**-OH	**2**	**3**	**4**	**5**-OH
Empirical formula	$C_{16}H_{17}FeNO_3$	$C_{28}H_{30}FeN_2O_4$	$C_{33}H_{37}FeN_3O_5$	$C_{38}H_{44}FeN_4O_6$	$C_{31}H_{35}Cl_2FeN_3O_5$
Formula weight	327.16	514.39	611.51	708.62	656.38
Space group	$P2_1$	$P2_12_12_1$	$C2$	$P2_1$	$P4_32_12$
a (Å)	7.4597(2)	10.1839(2)	26.190(5)	12.643(3)	11.4245(10)
b (Å)	8.9449(4)	10.7681(2)	6.4300(13)	6.4870(13)	
c (Å)	10.5661(5)	22.7514(2)	19.820(4)	21.397(4)	46.7497(40)
β (°)	98.509(2)		108.75(3)	98.40(3)	
V (Å^3)	697.28(5)	2494.95(7)	3160.6(11)	1736.1(6)	6101.7(5)
Z	2	4	4	2	8
D_{calc} (g cm^{-3})	1.558	1.369	1.285	1.356	1.429
Crystal size (mm)	$0.3 \times 0.2 \times 0.05$	$0.15 \times 0.10 \times 0.05$	$0.30 \times 0.10 \times 0.05$	$0.8 \times 0.5 \times 0.3$	$0.1 \times 0.2 \times 0.2$
μ (Mo–K_α) (cm^{-1})	10.90	51.46	5.21	4.87	7.1
Radiation (graphite monochromated in incident beam)	Mo–K_α	Cu–K_α	Mo–K_α	Mo–K_α	Mo–K_α
λ (Å)	0.71073	1.54060	0.71073	0.71073	0.71073
Reflections collected	2459	1420	4467	8782	43 578
Reflections observed	1297 [$I > 2\sigma(I)$]	553 [$I > 2\sigma(I)$]	1751 [$I > 2\sigma(I)$]	4317 [$I > 2\sigma(I)$]	6248 [$I > 2.5\sigma(I)$]
Goodness-of-fit	1.104	1.242	1.233	1.113	4.06
R, R_w [a]	0.0870, 0.1583	0.1008, 0.2325	0.0917, 0.1620	0.0588, 0.1329	0.075, 0.071

[a] $R = \Sigma(|F_o| - |F_c|)/\Sigma(|F_o|)$; $R_w = [\Sigma(w(|F_o| - |F_c|)^2/\Sigma(w|F_o|^2)]^{1/2}$.

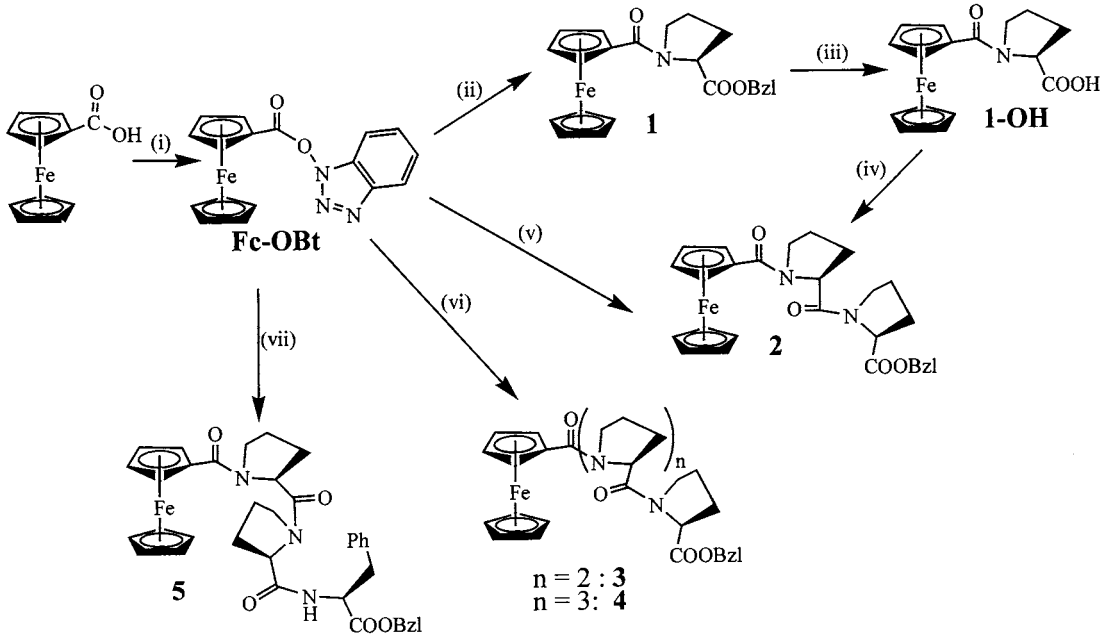

Scheme 1. Synthesis of ferrocenoyl-oligopeptides. (i) HOBt, DCC, (ii) H–Pro–OBzl, (iii) Pd/C, H_2, (iv) HOBt, DCC, H–Pro–OBzl, (v) H–Pro_2–OBzl, (vi) H–Pro_n–OBzl ($n = 3$, 4) and (vii) HOBt, DCC, H–Pro_2–Phe–OBzl.

used for all experiments. A phase-sensitive NOESY experiment was performed with 16 scans for each of 512 t1 increments. A spectral width of 4085 Hz was used in both dimensions with a mixing time of 400 ms and a relaxation delay of 2 s. Zero filling was applied to give a final matrix of 1×1 K. A shifted sine-squared window function was applied to both dimensions. A phase-sensitive TOCSY experiment was performed with 16 scans for each of 512 t1 increments. A spectral width of 4006 Hz was used in both dimensions with a mixing time of 80 ms and a relaxation delay of 2 s. Zero filling was applied to give a final matrix of 1×1 K. A shifted sine-squared window function was applied to both dimensions. A gradient-selected COSY was performed with four scans for each of 128 $t1$ increments. A spectral width of 4006 Hz was used in both dimensions. Zero filling was applied to give a final matrix of 1×1 K. A sine window function was applied to both dimensions. A gradient-selected phase-sensitive HSQC was performed with 16 scans for each of 512 $t1$ increments. The ^1H spectral width was 4006 Hz and the ^{13}C spectral width was 16 780 Hz. Zero filling was applied to give a final matrix of 2×1 K. A shifted sine-squared window function was applied to both dimensions. Gradient-selected HMBC experiments were performed with 480 scans for each of 128 t1 increments. The ^1H spectral width was 4006 Hz and the ^{13}C spectral width was 22 300 Hz. The delay for evolution of long-range couplings was set to 65 and 95 ms in separate experiments. Zero filling was applied to give a final matrix of 2×1 K. A Gaussian window function was applied in the ^1H dimension and a sine window function was applied in the ^{13}C dimension.

3. Results and discussion

3.1. Preparation of ferrocenoyl-oligoprolines

The syntheses of the Fc-oligoprolines are outlined in Scheme 1. We have explored two major routes for formation of Fc-peptides: (a) coupling of ferrocene carboxylic acid with the peptide and (b) stepwise build-up of the peptide chain on the organometallic fragment.

3.1.1. Coupling of the peptides with ferrocene carboxylic acid

All oligoprolines were synthesized from commercially available Boc–Pro–OH, H–Pro–OBzl·HCl (Bzl = benzyl) in CH_2Cl_2 solution following the standard carbodiimide protocol as described before [16]. After Boc deprotection, the peptides were coupled to ferrocenecarboxylic acid in CH_2Cl_2 using cyclohexylcarbodiimide (DCC) and hydroxybenzotriazole (HOBt) resulting in the clean formation of ether-soluble orange Fc–Pro_n–OBzl ($n = 2$–4, $Pro_2 = \mathbf{2}$, $Pro_3 = \mathbf{3}$, $Pro_4 = \mathbf{4}$). In a similar fashion, Fc–Pro_2Phe–OBzl (**5**) was prepared. Fc–Pro–OBzl (**1**) was obtained according to the literature procedure as a viscous brown oil [7]. There is not need to isolate the intermediate Fc–OBt. Instead, it was reacted in situ with the appropriate base-components. All products are obtained in yields ranging from 65–75%. All compounds are air and moisture stable in common solvents.

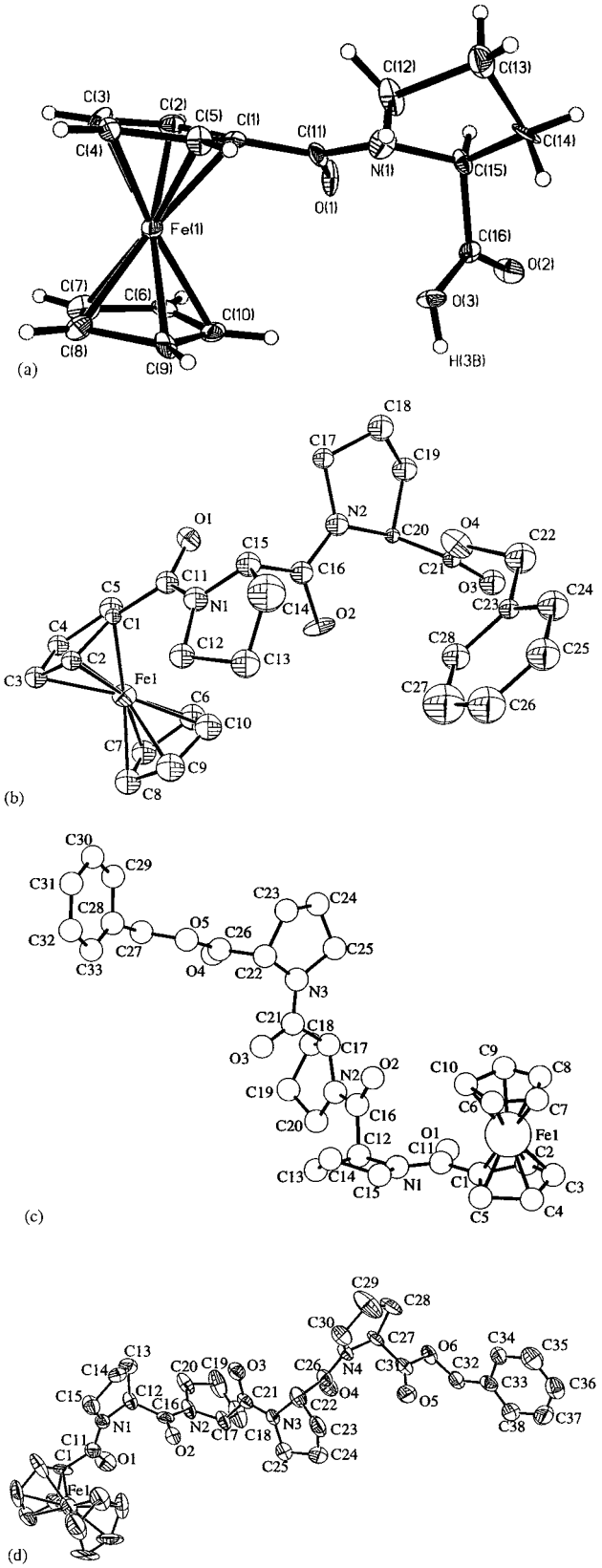

Fig. 1. Molecular structures of **1**-OH (a), **2** (b), **3** (c) and **4** (d). H atoms have been omitted in **2**–**4** for clarity. For **1**-OH, **2**, and **4** the thermal ellipsoids are at the 30% probability level.

3.1.2. Buildup of the peptide chain on the organometallic fragment

Alternatively, Fc–Pro–OBzl, obtained according to published procedures [7], can be used as a starting material for the stepwise addition of amino acids, as is demonstrated for **2**. The benzyl group in **1** can be conveniently removed by hydrogenation using 5% Pd/C in methanolic solution, resulting in the formation of the free acid Fc–Pro–OH (1-OH), which is obtained as a crystalline solid after recrystallization from CH_2Cl_2. **1**-OH was then coupled with H–Pro–OBzl·HCl to obtain **2** as a crystalline solid (see Section 2). All complexes were fully characterized by a combination of electrospray-MS (**1**–**5**), NMR spectroscopies (**1**–**5**), and X-ray crystallography (**1**-OH, **2**–**4**, **5**-OH).

3.2. Structural studies

In order to establish unequivocally the structure of the ferrocenoyl-oligoprolines, we carried out structural analyses by single-crystal X-ray crystallography of **1**-OH, **2**, **3**, **4**. Molecular structures of **1**-OH, **2**, **3** and **4** are shown in Fig. 1. Selected bond distances and angles for **1**-OH, **2**–**4** and **5**-OH are given in Table 2.

Complexes **2** and **3** crystallized as very thin needles, giving only poor-quality data, resulting in structures with high residuals. Hence, we cannot interpret the resulting structures for **2** and **3** in terms of bond lengths and angles. However, the quality of the data does allow us to analyze the structure of the peptide backbone. The geometries of the proline rings for **1**-OH, **2**–**4** and **5**-OH including their distances and angles are similar to other published peptide structures containing proline residues [11]. Furthermore, the distances and angles within the Fc moiety are similar to those observed for other Fc derivatives [8,12]. Typical for Fc-amides, the Cp and amide planes are virtually co-planar and only a small twist angles between the Cp and the amide planes for **1**-OH-**5** are observed (see Table 2), allowing electronic effects to be transmitted from the peptide to the ferrocene group [12]. Furthermore, the substituent does not influence the geometry of the ferrocene system and only a small Cp–Fe–Cp bent is observed [12].

Rather than discussing the geometries of each compound in detail, we wish to stress the common feature in all Fc–Pro$_n$–OBzl ($n = 2$–4) systems: in **2**–**4**, the oligoproline adopts a helical structure typical of polyproline II having exclusively *trans*-proline linkages with the ferrocenoyl moiety being part of the helix. The structure of polyproline II can be described as a left-handed helix with a translation of 3.12 Å per proline residue along the helical axis [13]. About three proline residues are needed to complete one full helical turn. For our four systems **1**-OH, **2**–**4** this means that in **3** the oligoproline chain has completed one full

Table 2
Selected bond distances (Å) and angles (°) for Fc–Pro–OH (**1**–OH), Fc–Pro_2–OBzl (**2**), Fc–Pro_3–OBzl (**3**), Fc–Pro_4–OBzl (**4**), Fc–Pro_2Phe–OH (**5**-OH)

	1-OH	**2**	**3**	**4**	**5**-OH
Bond distances					
av. Fe(1)–C_{Cp}	2.039(13)	2.04(4)	2.00(5)	2.030(7)	2.048(8)
av. Fe(1)–C_{CpR}	2.049(14)	2.06(3)	2.01(2)	2.034(6)	2.047(8)
O(1)–C(11)	1.257(14)	1.23(3)	1.222(12)	1.223(5)	1.244(9)
C(1)–C(11)	1.48(2)	1.50(4)	1.50(2)	1.489(6)	1.463(10)
C(11)–N(1)	1.314(14)	1.42(4)	1.362(14)	1.345(5)	1.369(8)
Bond angles					
O(1)–C(11)–N(1)	116.6(7)	117.0(32)	118.1(11)	120.1(4)	119.7(6)
Cp–Fe–Cp [a]	1.9	2.5	4.0	8.0	1.0
τ(Cp/amide) [b]	24.6	19.2	14.2	16.0	11.4

[a] Cp–Fe–Cp = bent angle.
[b] τ(Cp/amide) = dihedral angle between the substituted Cp ring plane and the amide plane.

helical turn. For **4**, the oligoproline has completed about 1 1/3 helical turns. In **1**-OH and **2**, the peptide has 1/3 and 2/3 of a helical turn completed, respectively. In other words, we have taken snapshots of a growing polyproline II chain.

The crystal structure of **5** is significantly different from that of the Fc–Pro_n–OR systems.

The ORTEP diagram of **5** is shown in Fig. 2, showing that the two Pro residues are connected in a *cis* fashion, followed by the Phe residue. A strong hydrogen bond between the Phe amide nitrogen N3 and O1 is typical for the structural motif of a β-turn (d(N···O) = 2.853 Å). NOESY-NMR studies in MeCN-d_6 confirm that the *cis*-proline linkage is preserved in solution as indicated by the correlation between α-H of Pro1 with β-H of Pro2.

At this point it must be pointed out that polyproline can exist in two forms, one with all peptide bonds being *cis* (polyproline I) and the all-*trans* form (polyproline II). Whereas the structure of polyproline II is a left-handed helix, polyproline I is a more compact all-*cis* right-handed helix with a translation of 1.85 Å [13]. Importantly, in solution, *cis*- and *trans*-polyprolines are in equilibrium with each other. The position of the equilibrium will depend on the polarity of the solvent, as shown by NMR experiments [14]. It was observed that less polar solvents will shift the equilibrium to favor *cis*-polyproline. We were concerned that different peptide structures may cause possible changes in the redox properties of the ferrocenoyl group and hence we had to ascertain the solution structure to ensure that it will be identical to the solid state structures.

Detailed NMR studies of two of the systems (**2** and **3**) were conducted in two solvents, $CDCl_3$ and MeCN-d_6. We were particularly interested in these solvents since they are typical for electrochemical measurements (vide infra). In the following we present in detail the results of an NMR study for **3** in $CDCl_3$. We have also

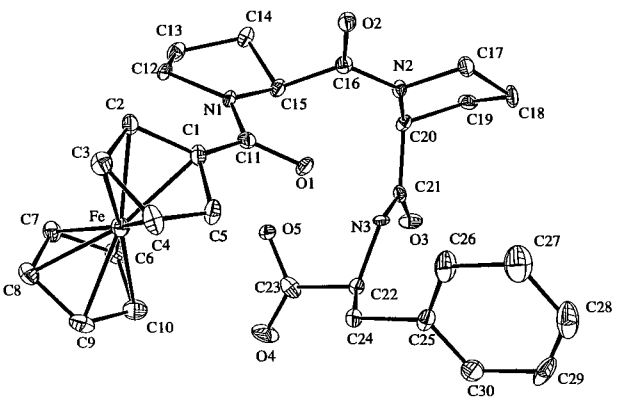

Fig. 2. ORTEP diagram for **5**. H atoms have been omitted for clarity. Thermal ellipsoids are at the 30% probability level. Compound **5** has a *cis*-proline linkage in contrast to the oligoprolines, resulting in the formation of a β-turn with a strong Fc–CO···NH_{Phe} hydrogen bond (see text).

carried out similar studies in MeCN-d_6, which are identical to those in $CDCl_3$. The structural assignment in solution is complicated by the chemical similarities among the protons of the three proline rings. The proton and carbon chemical shifts for **3** were assigned by analysis of DEPT-135, COSY, TOCSY (Fig. 3), HSQC (Fig. 4) and HMBC spectra.

The nomenclature used for the discussion of the assignments of the resonances in **3** is given in Scheme 2 and is identical to that used in the crystallographic analysis (see Fig. 1). The assignment of peaks is summarized in Table 3.

The assignment of the ferrocenoyl protons and the benzyl group is straightforward and is similar to other ferrocenoyl-peptides [17]. H6–10 give rise to a sharp singlet at δ 4.26 ($v_{1/2}$ = 5 Hz), which shows a clear correlation in the HSQC with a signal at δ 69.9 (C6–10). The broad signal at δ 4.33 ($v_{1/2}$ = 10 Hz), assigned to the two *meta*-protons of the substituted cyclopentadienyl (Cp) ring H3 and H4, correlates with the two

signals at δ 70.5 and 70.4 (C3 and C4). The two *ortho*-protons H2 and H5 give rise to two resonances at δ 4.83 (HSQC correlation with δ 71.5) and at δ 4.73 (HSQC correlation with δ 69.9).

The real challenge comes from the fact that all three proline residues in **3** are virtually indistinguishable by ordinary 1D NMR spectroscopy due to overlapping signals. However, all three are separated by an amide linkage thereby separating the three spin systems. 2D TOCSY allowed us to identify the three separate spin systems (see Fig. 3). Most decisively, the long-range ^{1}H, ^{13}C correlations detected in a 2D HMBC experiment allowed the assignment of the two carbonyl groups of the ferrocenoyl and ester groups, respectively. The resonance at δ 172.3 exhibits correlations with the benzyl protons (H27) at δ 5.13 and a CH proton at δ 4.62. Only the ester carbonyl group can give rise to this correlation pattern and it is therefore unequivocally assigned to C26. Based on this assignment, we can attribute the resonance at δ 4.62 to H22, which correlates in the HSQC spectrum with a signal at δ 59.0. As indicated by the TOCSY, the signal due to H22 is in the same spin system as the two signals at δ 3.79 and 3.60, which we assign to the two diastereotopic NCH_2 protons (H25). Both protons show a clear correlation in the HSQC with a signal at δ 46.8. Likewise, assignment of the carbonyl resonance at δ 169.6 to C11 is possible due to its HMBC correlation with two of the protons of the substituted Cp ring (H5) and to the CH resonance at δ 4.82, assigned to H12 (HSQC correlation to δ 59.5). This peak is TOCSY correlated with the NCH_2 resonances at δ 3.92 and 3.90 (H15). Having unequivocally assigned two proline rings, we are left with signals due to the central proline residue. By analogy, we assign the signal at δ 4.80 to H17 (HSQC correlation to δ 58.0, 135-DEPT negative). This signal is TOCSY correlated with the two diastereotopic NCH_2 signals at δ 3.92 and 3.71 (H20).

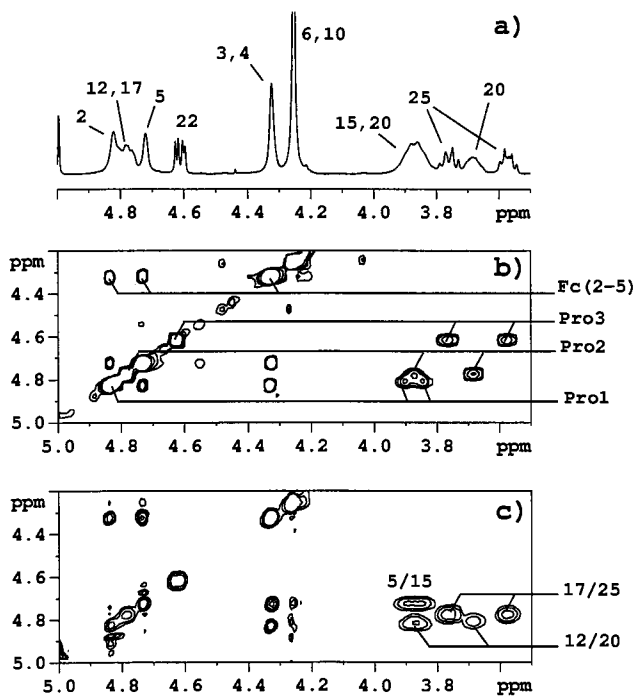

Fig. 3. Partial NMR spectra of **3** in the region of 5.00–3.65 ppm. (a) ^{1}H-NMR spectrum showing the assignment of all resonances using the labeling employed in Scheme 2. (b) 2D TOCSY spectrum showing the well-separated spin systems of the three proline residues and of the substituted cyclopentadienyl ring. (c) 2D NOESY spectrum showing cross peaks between H5 of the Cp ring and the Hs of the NCH_2 group (site 15), between sites 17 and 25 and between sites 12 and 20, confirming the overall structure to be equivalent to that observed in the solid state (all-*trans*-Fc–Pro_3–OBzl).

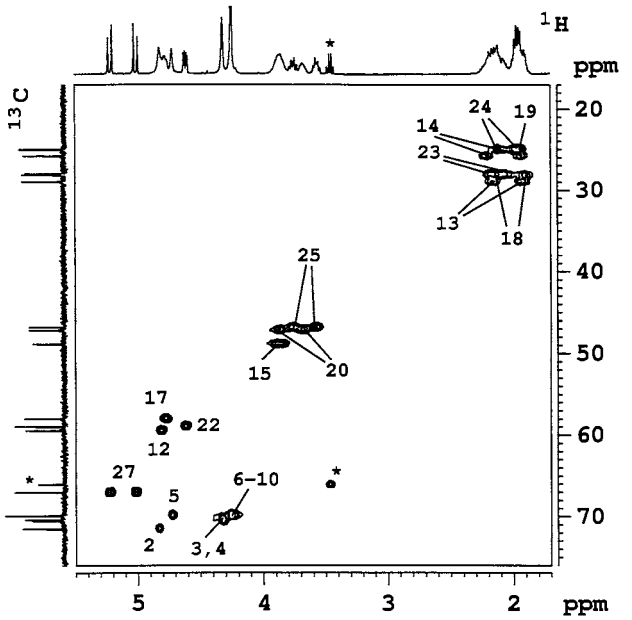

Fig. 4. 2D HSQC spectrum of **3** (labeling is according to Scheme 2).

The NOESY spectrum (Fig. 3) shows several noteworthy correlations. The Cp proton H5 and the CH H15 of the first proline ring show a strong NOE signal. Furthermore, the CH signals H12 and H17 show NOE peaks to H20 and H25, respectively. This 'α-H to δ-H' correlation pattern is typical for a *trans*-proline helix [14]. It is important to point out that NOE cross peaks for 'α-H to α-H' CH/CH interactions are not observed, demonstrating the absence of the all-*cis* conformer.

It is also interesting to note the absence of any discernible NOE of H27, which is most likely due to the lack of any preferred conformation for the benzyl group. It must be pointed out that in MeCN-d_6, we observed the identical NOESY spectrum with respect to the oligoproline, indicating that the secondary peptide structure is identical to that in $CDCl_3$.

To summarize the NMR studies: the solution and solid state peptide structures are identical. The NOESY spectra for **2** and **3** show a correlation between α-H and

Table 3
Peak assignments for Fc–Pro_3–OBzl. The atom labels are given in Scheme 2 and are identical to those used in Fig. 1. All shifts (δ) are given in ppm

Site	^{1}H	^{13}C [a]	HSQC	HMBC	NOESY
1		76.5			
2	4.83		71.5		
3, 4	4.33		70.4/5		
5	4.73		69.9		5 to 15
6–10	4.26		69.9		
11	–	169.6		2, 5, 12	
12	4.82		59.5		12 to 20
13	2.20, 1.97		29.0		
14	2.45, 1.97		25.8		
15	3.92, 3.90		48.9		15 to 5
16					
17	4.80		58.0		17 to 25
18	2.21, 2.13		28.0		
19	2.02, 2.01		25.0		
20	3.92, 3.71		47.2		20 to 12
21					
22	4.62		59.0		
23	2.17, 1.94		28.2		
24	2.16, 2.02		25.1		
25	3.79, 3.60		46.8		25 to 17
26	–	172.3		22, 27	
27	5.13, 5.30		67.0	33, 29	
28	–	135.9			
29–33	7.35		128.7, 128.5, 128.4		

[a] ^{13}C resonances given for those carbonyl carbons and quaternary carbon atoms. For all other carbon atoms the HSQC and ^{13}C signal are at identical chemical shifts.

δ-H of two neighboring proline rings exclusively, as would be expected for an all-*trans* arrangement. Although facile solvent-dependent interconversion between *cis*- and *trans*-oligoprolines is well known [14], we have no evidence to suggest isomerization in our Fc-oligoprolines in solution. No NOESY cross peaks corresponding to *cis*-proline linkages are observed in $CDCl_3$ and in MeCN-d_6.

3.3. Electrochemistry

Next, we proceeded to investigate the redox chemistry of the ferrocenoyl-peptides **1**-OH, **2**–**4**, and **5**-OH. Expectedly, the cyclic voltammograms of **1**-OH, **2**–**4**, and **5** measured in dry acetonitrile using a glassy carbon working electrode, show a single quasi-reversible one-electron oxidation wave. Importantly, the redox properties of the Fc moiety are dependent on the length and structure of the oligoproline chain. With growing proline chain length, the molecule becomes easier to oxidize (Table 4, Fig. 5).

Whereas Fc–Pro–OR (R = H, Bzl) is reversibly oxidized at 165 ± 6 mV (vs. Fc/Fc^+), **2** undergoes oxidation at $E_{1/2} = 150 \pm 7$ mV (vs. Fc/Fc^+). It is important to keep in mind that two prolines in **2** are insufficient to complete a full helical turn. Extending the chain by an additional proline residue as in **3** and thereby completing a full helical turn causes the redox potential to shift to 140 ± 5 mV (vs. Fc/Fc^+). In **4**, further extension of the chain by an additional proline residue does not result in a significant change of the redox potential of the molecule.

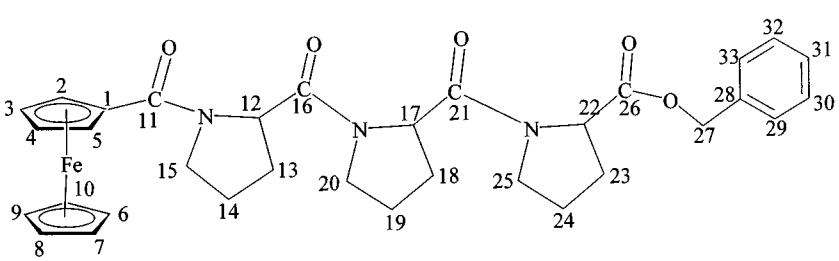

Scheme 2. Structure of **3**, explaining the labeling pattern used in Figs. 3 and 4.

Table 4
Electrochemical properties of ferrocenoyl-peptides

Compound	$E_{1/2}$ (mV) [a,b]	$E_p^a - E_p^c$ (mV)
Fc–Pro–OBzl (**1**)	165 ± 6	85
Fc–Pro–OH (**1**-OH)	170 ± 5	83
Fc–Pro_2–OBzl (**2**)	150 ± 7	82
Fc–Pro_3–OBzl (**3**)	140 ± 5	80
Fc–Pro_4–OBzl (**4**)	140 ± 5	80
Fc–Pro_2Phe–OBzl (**5**)	170 ± 5	81
Fc–Pro_2Phe–OH (**5**-OH)	169 ± 6	84

[a] $E_{1/2}$ vs. internal ferrocene/ferrocenium couple (440 mV vs. SCE in MeCN with peak separation of 80 mV).
[b] All measurements were carried out at a scan rate of 100 mV s^{-1}.

Whereas the redox potential of the $(H_3N)_5Os$-moiety in pyridine-linked $(H_3N)_5Os$-oligoprolines [5a] is not influenced by the chain length of the oligoproline as shown by Isied and coworkers, the redox potentials of **1**-OH, and **2**–**4** are clearly dependent on the oligoproline chain length or structure. This difference is most likely related to the rotational freedom of the $(H_3N)_5Os$-group about the Os–N linkage in solution (see Scheme 3).

In contrast, the Fc group is restricted with respect to rotation about the amide linkage and exists in two conformations in solution, as confirmed by 2D NOESY studies in acetonitrile solution which show a cross peak for both of the *ortho*-Hs of the substituted Cp ring to the δ-H of Pro1. The energy barrier for rotation about the amide linkage was estimated to be 35–40 kJ mol^{-1} [12]. In both conformations the interaction between the two π-systems of the Cp and the amide groups is maximized. We do not observe any significant influence of the benzyl-protecting group on the redox potential of the Fc-group.

We were surprised to find that **5** is significantly more difficult to oxidize than **3** (Table 4). Clearly, the Fc-moiety is able to 'sense' the presence of the third amino acid in the chain. As the redox potentials show, we are able to differentiate between a proline and a non-proline amino acid. It is tempting at this point to speculate about the ability of the Fc-moiety to distinguish between the two structural motifs present in **1**–**4** and **5**. However, in order to draw a firm conclusion about the ferrocene's ability to recognize structural features, it is clear that we will have to investigate a larger number of systems.

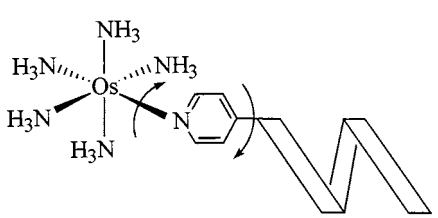

Scheme 3. Rotational freedom around the Os–py and py–peptide bond in Isied's $(H_3N)_5Os$–py–peptides (see Ref. [5a]).

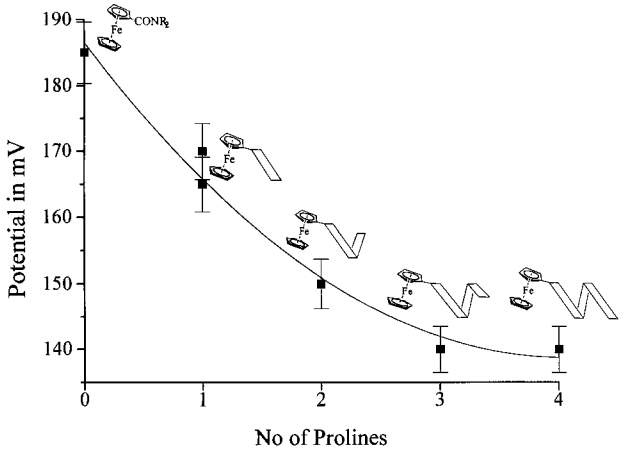

Fig. 5. Electrochemical properties of Fc–Pro_n–OBzl (for details see Table 4). Potentials were recorded using a glassy carbon electrode in MeCN vs. the ferrocene/ferrocenium couple as internal standard using $^nBu_4NClO_4$ (0.1 M) as supporting electrolyte.

It is important to emphasize that upon increasing the peptide chain length, the ferrocenoyl group becomes easier to oxidize. Due to the helical structures exhibited by the Fc-oligoprolines **1**–**4** all carbonyl groups point towards the carboxy terminus of the peptide chain, thereby creating a permanent dipole moment with the Fc-moiety being at the positive end of the dipole [5l,m]. An increase in the length of the peptide should result in an increased dipole moment. In light of the aforementioned, the observed drop of redox potentials of the Fc–Pro_n–OBzl series is counterintuitive in that it is expected that the oxidation should become more difficult with an increased chain length. The Fc-moiety is at the positive end of the dipole, yet increasing the oligoproline chain leads to a relative stabilization of the Fc^+. Our results are different from those reported by Fox who explains variations in ET rates in much longer helical Aib-rich peptides in terms of electric field effects created by the alignment of all carbonyl groups within the peptide [5l,m,15]. This suggests that factors other than electric field effects caused by the peptide's dipole are influencing the redox potentials our Fc–Pro_n–OBzl systems. Theoretical studies [12] on model systems containing the Fc group suggest that the directional character of an oxygen p-orbital perpendicular to the Cp/amide plane creates a spatial anisotropy of the electron distribution in the molecule and may be partly responsible for the observed electronic effect.

4. Conclusions

In the present study, we have described the facile synthetic pathway to peptides possessing the redox-active ferrocenoyl group at the N-terminus of the peptide.

Structural studies of the Fc-oligoproline **1**-OH, **2**–**4** show that all systems possess a left-handed polyproline II helix. Our Fc–Pro_n–OR series presents snapshots of the growing left-handed polyproline II helix. Importantly, this structure is maintained in acetonitrile solution. Electrochemical measurements carried out in dry acetonitrile solution show for the first time that the redox potential of a redox probe attached to a peptide chain is influenced by the number of amino acid residues and its composition. Our results suggest that the Fc-moiety is able to 'sense' the presence of the third amino acid in the chain. The presence of non-proline amino acids as in **5**, has structural effects, causing a change in the secondary structure of the peptide, which may suggest that the Fc-group is in fact sensing a structural change of the peptide. This may allow us to develop the ferrocenoyl group as an electrochemical sensor to probe the local structure in a more complex peptide or even protein. However, at present our results are not representative and a more detailed study of a large number of structurally varied Fc-peptides must be investigated in order to draw firm conclusions. We will investigate this effect in detail by synthesizing a series of structurally diverse Fc-substituted peptides and by studying their electrochemical behavior in solution and supported on surfaces.

5. Supplementary material

Crystallographic data for the structural analyses have been deposited with the Cambridge Crystallographic Data Centre: CSD-114495 for compound **1**, CSD-114496 for compound **2**, CSD-114497 for compound **3**, CSD-114543 for compound **4** and CSD-114544 for compound **5**. Copies of this information may be obtained free of charge from: The Director, CCDC, 12 Union Road, Cambridge CB2 1EZ (fax: +44-1223-336-033 or e-mail: deposit@ccdc.cam.ac.uk or www:http//www.ccdc.cam.ac.uk).

Acknowledgements

This work was supported in part by the Samuel and Ethel Brown Memorial Fund and in part by the Department of Chemistry, University of Saskatchewan. H.B.K. is the recipient of the University of Saskatchewan's NSERC President's award.

References

[1] I. Bertini, H.B. Gray, S.J. Lippard, J.S. Valentine, Bioinorganic Chemistry, University Science Books, Mill Valley, CA, 1994.

[2] (a) M. Meier, R. van Eldik, I.-L. Chang, G.A. Mines, D.S. Wuttke, J.R. Winkler, H.B. Gray, J. Am. Chem. Soc. 116 (1994) 1577. (b) D.S. Wuttke, H.B. Gray, S.L. Fisher, B. Imperiali, J. Am. Chem. Soc. 115 (1993) 8455. (c) I.-J. Chang, H.B. Gray, J.R. Winkler, J. Am. Chem. Soc. 113 (1991) 7056. (d) D.S. Wuttke, M.J. Bjerrum, J.R. Winkler, H.B. Gray, Science 256 (1992) 1007. (e) O. Farver, I. Pecht, Proc. Natl. Acad. Sci. USA 86 (1989) 6968. (f) O. Farver, I. Pecht, J. Am. Chem. Soc. 114 (1992) 5764. (g) O. Farver, L.K. Skov, G. Gilardi, G. van Pouderoyen, G.W. Canter, S. Wherland, I. Pecht, Chem. Phys. 204 (1996) 271. (h) C.C. Moser, J.M. Keske, K. Warncke, R.S. Farid, P.L. Dutton, Nature 355 (1992) 796. (i) R.S. Farid, C.C. Moser, P.L. Dutton, Curr. Opin. Struct. Biol. 3 (1993) 225.

[3] (a) D.N. Beratan, J.N. Belts, J.N. Onuchic, Science 252 (1991) 1285. (b) S.S. Skourtis, D.N. Beratan, J. Biol. Inorg. Chem. 2 (1997) 378.

[4] R. Langen, J.L. Colon, D.R. Casimiro, T.B. Karpishin, J.R. Winkler, H.B. Gray, J. Biol. Inorg. Chem. 1 (1996) 221.

[5] (a) S.S. Isied, Chem. Rev. 92 (1992) 381. (b) K.S. Schanze, K. Sauer, J. Am. Chem. Soc. 110 (1988) 1180. (c) M. Sisido, R. Tanaka, Y. Inai, Y. Imanishi, J. Am. Chem. Soc. 111 (1989) 6790. (d) M. Farragi, M.R. DeFelippis, M.H. Klapper, J. Am. Chem. Soc. 111 (1989) 5141. (e) M.R. DeFilippis, M. Faraggi, M.H. Klapper, J. Am. Chem. Soc. 112 (1990) 5640. (f) G. Basu, M. Kubasik, D. Angelos, B. Secor, A. Kuki, J. Am. Chem. Soc. 112 (1990) 9410. (g) S.L. Mecklenburg, B.M. Peek, B.W. Erickson, T.J. Meyer, J. Am. Chem. Soc. 113 (1991) 8540. (h) S.L. Mecklenburg, B.M. Peek, J.R. Schoonover, D.G. McCafferty, C.G. Wall, B.W. Erickson, T.J. Meyer, J. Am. Chem. Soc. 115 (1993) 5479. (i) A.K. Mishra, R. Chandrasekar, M. Faraggi, M.H. Klapper, J. Am. Chem. Soc. 116 (1994) 1414. (j) T. Hayashi, T. Takimura, Y. Hitomi, T. Ohara, H. Ogoshi, J. Chem. Soc. Chem. Commun. (1995) 545. (k) G. Jones, Z. Feng, C. Oh, J. Phys. Chem. 99 (1995) 3883. (l) E. Galoppini, M.A. Fox, J. Am. Chem. Soc. 118 (1996) 2299. (m) M.A. Fox, E. Galoppini, J. Am. Chem. Soc. 119 (1997) 5277.

[6] (a) For a recent survey see: P.D. Beer, J. Chem. Soc. Chem. Commun. (1996) 689. (b) Z. Chen, A.R. Graydon, P.D. Beer, J. Chem. Soc. Faraday Trans. 92 (1996) 97. (c) Also see: E.C. Constable, Angew. Chem. Int. Ed. Engl. 30 (1991) 407.

[7] H.-B. Kraatz, J. Lusztyk, G.D. Enright, Inorg. Chem. 36 (1997) 2400.

[8] (a) T. Okamura, K. Sekauye, N. Ueyama, A. Nakamura, Inorg. Chem. 37 (1998) 6731. (b) I.R. Butler, S.C. Quale, J. Organomet. Chem. 552 (1998) 63. (c) J. Zakrzewski, A. Klys, M. Bukowska-Strzyzewska, A. Tosik, Organometallics 17 (1998) 5880.

[9] SHELXTL, Version 5; Siemens Energy & Automation, Inc., 1994.

[10] (a) E.J. Gabe, Y. Le Page, J.-P. Charland, F.L. Lee, P.S. White, J. Appl. Crystallogr. 22 (1989) 384. (b) Y. Le Page, E.J. Gabe, J. Appl. Crystallogr. 12 (1979) 464.

[11] (a) T. Kojima, I. Tanaka, T. Ashida, Acta Crystallogr. Sect. B 38 (1982) 221. (b) M.E. Kamwaya, O. Oster, H. Bradaczek, M.N. Ponnuswamy, S. Parthasarathy, R. Nagaraj, R., P. Balaram, Acta Crystallogr. Sect. B 38 (1982) 172. (c) M.N. Sabesan, K. Venakatesan, Acta Crystallogr. Sect. B 27 (1971) 1879. (d) T. Ueki, T. Ahida, M. Kakudo, Acta Crystallogr. Sect. B 27 (1971) 2219.

[12] L. Lin, A. Berces, H.-B. Kraatz, J. Organomet. Chem. 556 (1998) 11.

[13] (a) I.Z. Steinberg, W.F. Harrington, A. Berger, M. Sela, E. Katchalski, J. Am. Chem. Soc. 82 (1960) 5263. (b) J. Engel, Biopolymers 4 (1966) 945. (c) P.R. Schimmel, P.J. Flory, Proc. Nat. Acad. Sci. 58 (1967) 52. (d) P.M. Cowan, S. McGavin, Nature (London) 176 (1955) 501. (e) W. Traub, U. Schmueli, Nature (London) 195 (1963) 1165. (f) R.E. Burge, Harrison, S. McGavin, Acta Crystallogr. 15 (1962) 914.

[14] (a) H.C. Chiu, R. Bersohn, Biopolymers 16 (1977) 277. (b) H.N. Cheng, F.A. Bovey, Biopolymers 16 (1977) 1465. (c) Y.-Y.H. Chao, R. Bersohn, Biopolymers 17 (1978) 2761 and Refs. therein. (d) C.M. Deber, F.A. Bovey, J.P. Carver, E.R. Blout, J. Am. Chem. Soc. 92 (1970) 6191. (e) See also Ref. [5m]

[15] Fox cites the electrical dipole generated to be ca. 10^9 V m^{-1} (see also Refs. [5l,m]).

[16] M. Bodanszky, A. Bodanszky, The Practice of Peptide Synthesis, 1st ed., Springer–Verlag, Berlin, 1984.

[17] P. Saweczko, H.B. Kraatz, Coord. Chem. Rev. (1999) in press and Refs. therein.